
Nonlinear Oscillations and Chaos from Digital Filter Overflow

Anthony C. Davies

Phil. Trans. R. Soc. Lond. A 1995 **353**, 85-99

doi: 10.1098/rsta.1995.0092

Email alerting service

Receive free email alerts when new articles cite this article - sign up in the box at the top right-hand corner of the article or click [here](#)

To subscribe to *Phil. Trans. R. Soc. Lond. A* go to:

<http://rsta.royalsocietypublishing.org/subscriptions>

Nonlinear oscillations and chaos from digital filter overflow

BY ANTHONY C. DAVIES

*Department of Electronic and Electrical Engineering, King's College,
University of London, Strand, London WC2R 2LS, UK*

Nonlinear digital-filter overflow-oscillations arising from two's complement arithmetic are described with the emphasis on explaining the reasons for the behaviour and providing illustrations of typical oscillations. The complex properties of some of these oscillations have led to extensive investigations of the nonlinear dynamics and to proposals for applications. The paper provides an introduction to the published literature on this subject.

1. Introduction

Digital filters are increasingly used for processing discrete-time (sampled-data) signals, and integrated-circuit technology has made available low-cost implementations for many applications in communications and control, using software, hardware or programmable digital signal processors fabricated as a VLSI chip.

Mathematically, digital filters are difference equations, which, for most applications, are linear with constant coefficients. The input–output behaviour of a filter of order n comprises an n th order difference equation from which structures made of adders, delays and multipliers may be derived. A set of first order difference equations, involving n state variables, provides a basis for description and analysis of most aspects of such structures.

The processing is commonly subdivided into a cascade of simpler structures, with second-order ones preferred for many applications. Often, the structures involve recursion (i.e. feedback) with the consequent risk of instability if coefficients are incorrectly chosen. The analysis and design of such filters can mostly be carried out within a framework of linear algebra. The theory, techniques, terminology and design procedures are now well established (Roberts 1987), with the z -transform providing a major tool.

However, for digital implementation, both signals and coefficients must in practice be represented by a finite number of binary digits (commonly 16 or 32 in current practice) and the mathematical operations (either floating or fixed point arithmetic) involve nonlinearities (rounding or truncation errors and the possibility of overflow and underflow).

These inevitable finite-wordlength effects cause deviations from ideal behaviour and can result in oscillations from a filter structure which would otherwise be stable.

The usual fixed-point implementation uses two's complement arithmetic. This arithmetic has a highly nonlinear overflow characteristic which can give rise to large amplitude oscillations in recursive structures. Such oscillations can easily be sup-

Phil. Trans. R. Soc. Lond. A (1995) **353**, 85–99

Printed in Great Britain

© 1995 The Royal Society

T_EX Paper

pressed in second-order filters (and many higher-order ones) either by a simple modification to the overflow characteristic (Ebert *et al.* 1969) or by using only special structures guaranteed to be free of such oscillations (Barnes & Fam 1977; Roberts 1987). The oscillations are therefore seldom a problem in real applications, but they are of intrinsic interest because of their complex dynamics and because applications for them have been proposed (Kutzer *et al.* 1994). Oscillations can also arise from rounding or truncation nonlinearities (Butterweck *et al.* 1989; Laakso 1993) but are outside the scope of this paper.

Since it was pointed out that they could form a complex, fractal, pattern in the state space (Chua & Lin 1988), the oscillations have been studied in detail (Davies & Sriranjjan 1989; Chua & Lin 1990*b*; Ogorzałek *et al.* 1992; Galias & Ogorzałek 1992; Wu & Chua 1993; Kocarev & Chua 1993; Davies 1994), but there remain many unanswered questions, and most of the quoted studies have considered only one or a few specific coefficient values.

Most investigations ignore other inevitable nonlinear effects arising from the finite wordlength of the signal samples, so the analysis is strictly not a study of digital filters but of analogue sampled-data filters with a sawtooth nonlinearity in a feedback path. This makes mathematical analysis tractable, and enables many properties of these oscillations to be determined, but leads to some conclusions which do not apply to real digital filters, and not all properties of the actual overflow oscillations can be accounted for by such an analysis.

2. Review of linear theory and notation

The zero-input state equations of a second-order direct-form digital filter are:

$$\mathbf{x}_{k+1} = \begin{bmatrix} x_1 \\ x_2 \end{bmatrix}_{k+1} = \begin{bmatrix} 0 & 1 \\ b & a \end{bmatrix} \begin{bmatrix} x_1 \\ x_2 \end{bmatrix}_k = \mathbf{A}\mathbf{x}_k, \quad k = 0, 1, 2, \dots$$

k denotes the discrete-time step. For stability, the eigenvalues of \mathbf{A} must be within the unit circle, which is the interior of a triangle PQR in the coefficient (a, b) plane (figure 1). In the region below the parabola $b = -a^2/4$ there are two complex-conjugate eigenvalues. For eigenvalues at radius r and angles $\pm\theta$, $b = -r^2$ and $a = 2r \cos \theta$. The state equations are then:

$$\mathbf{x}_{k+1} = \begin{bmatrix} 0 & 1 \\ -r^2 & 2r \cos \theta \end{bmatrix} \mathbf{x}_k.$$

Radius r is a measure of damping. If $r = 1$, the structure is a lossless resonator (digital oscillator) and generates a sampled sinusoidal signal. Angle θ determines the samples per period. For $r < 1$, the sinusoid has an exponentially decaying envelope, while for $r > 1$, the structure is unstable, with an exponentially increasing envelope.

Figure 2 illustrates typical trajectories. If $r = 1$, orbits on an ellipse are generated. If $g\theta = h\pi$ for some integers, g, h , a finite number of points form the orbit, whereas if θ/π is irrational, the points are dense on the ellipse.

Analysis is simplified by a non-singular transformation, $\mathbf{x} = \mathbf{T}\mathbf{w}$, of the state variables to a new plane, \mathbf{w} . The ellipses become circles, and if $r = 1$, at each transition the state moves through an angle of θ at constant radius, as illustrated in

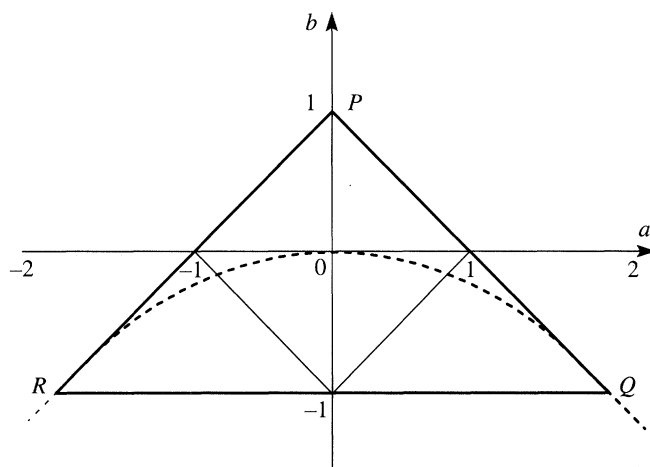
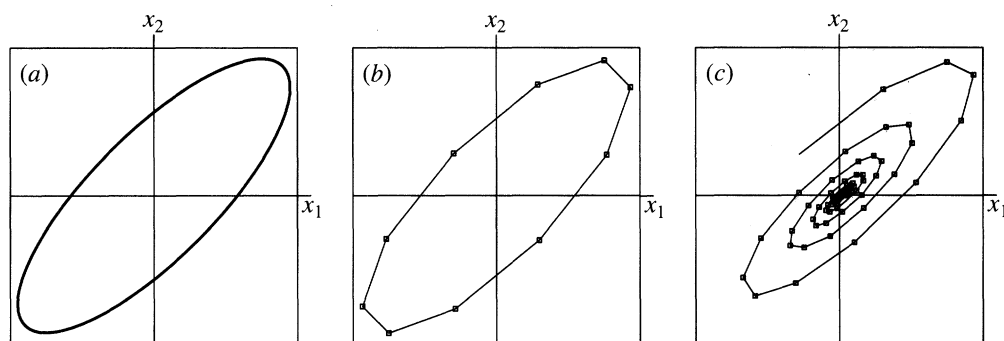
Figure 1. Stability triangle in the (a, b) coefficient plane.Figure 2. (a) Trajectory for $r = 1$ and irrational θ/π ($\theta = 36.23^\circ$, $x_0 = [0.29, -0.29]^T$). (b) Trajectory for $r = 1$ and rational θ/π ($\theta = 36^\circ$, $x_0 = [0.29, -0.29]^T$). (c) Trajectory with $r < 1$, $\theta = 36^\circ$.

figure 3.

$$T = \begin{bmatrix} 1 & 0 \\ r \cos \theta & r \sin \theta \end{bmatrix} \quad T^{-1} = \frac{1}{\sin \theta} \begin{bmatrix} \sin \theta & 0 \\ -\cos \theta & 1/r \end{bmatrix}$$

and

$$w_{k+1} = T^{-1}ATw_k$$

3. The overflow nonlinearity

Signals are assumed normalized to $[-1, +1)$, with overflow outside this range defined by nonlinearity F ,

$$F[u] = (u + 1) \bmod 2 - 1,$$

less satisfactorily expressed as $F[u] = u - 2i$ for $2i - 1 \leq u < 2i + 1$ where i is an integer. This is an idealization of suitably scaled fixed-point binary arithmetic, in which the largest positive and negative representable numbers using d bits are, respectively, $+(2^{d-1} - 1)/2^{d-1}$ (= binary $0.1111\dots$) and -1 (= binary $1.0000\dots$). Thus, -1 can

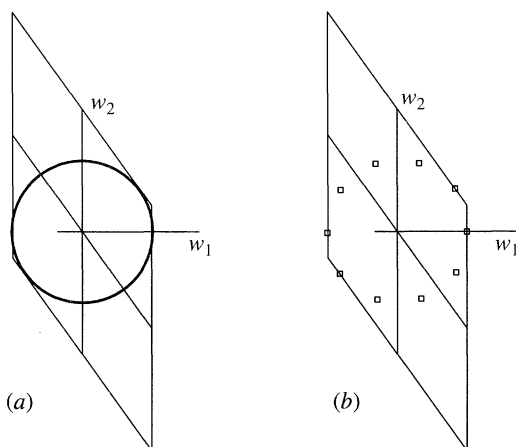


Figure 3. Trajectories in w -plane: (a) $r = 1$, $\theta = 36.23^\circ$; (b) $r = 1$, $\theta = 36^\circ$.

be represented exactly but $+1$ cannot. The sloping parts of the nonlinearity are in reality a linear ‘staircase’ with 2^d steps, but this quantization is neglected and, in effect, d is assumed to be infinite. Some consequences of this idealization are discussed in §8.

Because of the nonlinearity, the state space is restricted to a square:

$$I^2 : -1 \leq x_1, x_2 < +1.$$

Any transition which results in overflow is associated with an upward or downward ‘jump’ of 2 in the x_2 state variable to bring the state back into I^2 . In the direct-form structure x_1 cannot overflow because $x_{1(k+1)} = x_{2(k)}$. For other structures, this would not necessarily be the case. The system is thus a piecewise-linear map $F : I^2 \rightarrow I^2$. Since F is *onto* and \mathbf{A} is non-singular (except for $r = 0$), F^{-1} exists. For $r \leq 1$, F is *one-to-one* (see Appendix).

The nonlinear behaviour is equivalent to driving the linear system by a ternary $\{+2, -2, 0\}$ sequence and the state equations for the filter with overflow may therefore be expressed as:

$$\mathbf{x}_{k+1} = F[\mathbf{A}\mathbf{x}_k] = \mathbf{A}\mathbf{x}_k + \mathbf{b}s_k,$$

$$\begin{bmatrix} x_1 \\ x_2 \end{bmatrix}_{k+1} = \begin{bmatrix} 0 & 1 \\ -r^2 & 2r \cos \theta \end{bmatrix} \begin{bmatrix} x_1 \\ x_2 \end{bmatrix}_k + \begin{bmatrix} 0 \\ 2 \end{bmatrix} s_k,$$

and in reverse-time:

$$\mathbf{x}_{k-1} = F^{-1}[\mathbf{A}\mathbf{x}_k] = \mathbf{A}^{-1}\mathbf{x}_k + \begin{bmatrix} 2 & 0 \end{bmatrix}^T s_{k-1}.$$

An overflow oscillation is thus associated with \mathbf{s} ($= s_k$, $k = 0, 1, 2, \dots$), a ternary sequence of $+1, -1, 0$ values representing the overflows.

If Σ denotes the set of all infinite sequences over the alphabet $\{+, -, 0\}$, then admissible sequences (those which correspond to possible overflow oscillations) are a subset Σ_F of Σ . Denoting by S the map from states \mathbf{x} in I^2 to sequences in Σ , the inverse map is defined by

$$S^{-1}(\mathbf{s}) = \{\mathbf{x} \in I^2 : S(\mathbf{x}) = \mathbf{s}\}.$$

Identifying admissible and non-admissible ternary sequences and determining their structure and periodic lengths are challenging theoretical problems, so far only partially solved. The sequences provide the foundation for a description in terms of symbolic dynamics using symbols $\{+, -, 0\}$.

In the w -plane, the state space, J^2 , is a rhombus for $r = 1$, with sides $2/\sin\theta$, interior angle θ , and inscribed circle C of unit radius. Each state transition in J^2 is a clockwise rotation through θ followed in the case of overflow by a vertical jump of $\pm 2/\sin\theta$ to return to the interior of J^2 .

The positive and negative overflows partition I^2 into three regions I_1, I_0, I_{-1} with boundaries:

$$B_1 : -r^2x_1 + 2r \cos\theta x_2 = 1,$$

$$B_{-1} : -r^2x_1 + 2r \cos\theta x_2 = -1.$$

In the J^2 partition into J_1, J_0, J_{-1} , for $r = 1$ the boundaries are tangents to C and their slope is $-\cot 2\theta$. I_0, J_0 are the regions in which $\mathbf{A}\mathbf{x}_0$ does not overflow (e.g. $s_0 = 0$), while I_1, J_1 and I_{-1}, J_{-1} are triangular regions in which $\mathbf{A}\mathbf{x}_0$ overflows in the positive and negative direction, respectively.

(In the non-typical case of a linearly unstable filter with (a, b) values large enough overflow-jumps of multiples of 2 become possible and \mathbf{s} must then be modified accordingly to a $(2m + 1)$ level sequence ($m > 1$.)

4. Overflow oscillations

Figure 4 shows typical overflow oscillations from a lossless resonator ($r = 1$); \mathbf{s} is of period 3 (+−0) and period 17 (+−00+−00+−0+−0+−0). Joining successive states by a line shows how the trajectory is formed. Although \mathbf{s} is periodic, the overflow oscillation generally is not. However, in each case, a periodic oscillation does exist, generated if the initial state is at the centre of one of the ellipses (or circles, in J^2). If r is infinitesimally less than one, the oscillation converges to a limit cycle with the same period as \mathbf{s} (figure 5). The oscillation which occurs depends critically upon the initial state \mathbf{x}_0 .

(a) The circle formation process

Consider an oscillation of period m , and initial state \mathbf{w}_0 at the centre of one of the m circles. Let $v = 2/\sin\theta$ (the magnitude of the vertical jump following an overflow). By representing each state \mathbf{w} as a complex number (e.g. J^2 as an argand diagram with axis w_2 as the imaginary axis):

$$\mathbf{w}_1 = \mathbf{w}_0 e^{-j\theta} + js_0 v,$$

$$\mathbf{w}_2 = \mathbf{w}_1 e^{-j\theta} + js_1 v,$$

$$\dots$$

$$\mathbf{w}_m \equiv \mathbf{w}_0 = \mathbf{w}_{m-1} e^{-j\theta} + js_{m-1} v.$$

If \mathbf{w}_0 is perturbed slightly to \mathbf{w}'_0 by a small distance and angle:

$$\mathbf{w}'_0 = \mathbf{w}_0 + d e^{j\phi},$$

$$\dots$$

$$\mathbf{w}'_m = \mathbf{w}_m + d e^{-jm\theta+j\phi} = \mathbf{w}_0 + d e^{-jm\theta+j\phi}.$$

Thus, on return to the vicinity of \mathbf{w}_0 the deviation is unchanged in magnitude, and the angle has changed to $\phi - m\theta$. Since θ/π is irrational, the oscillation is no

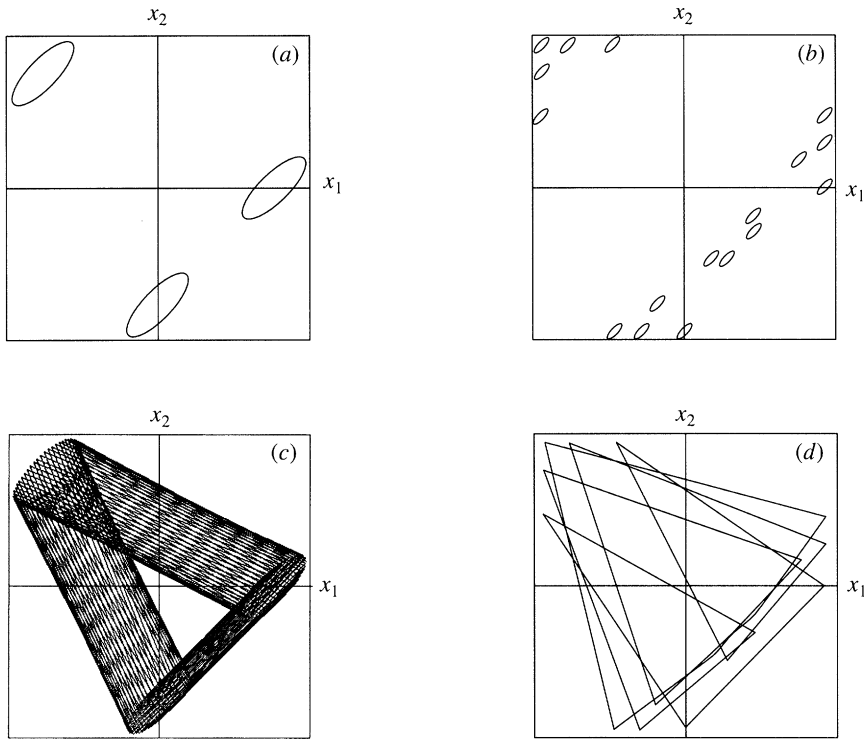


Figure 4. Overflow oscillations: (a) $r = 1$, $\theta = 36.23^\circ$, $x_0 = [0.7, -0.7]^T$; (b) $r = 1$, $\theta = 36.23^\circ$, $x_0 = [0.93, -0.93]^T$; (c) as (a) but states joined by lines; (d) as (b) but states joined by lines and $x_0 = [0.946, -0.946]^T$.

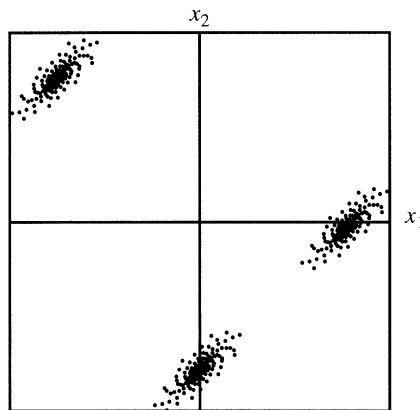


Figure 5. Period 3 limit cycle with $s = \{\dots 0 + -0 + -0 + -\dots\}$.

longer periodic and forms a dense set of points on a circle of radius d around each of the original states. The ternary sequence s is unchanged.

The deviation, d , may be increased until one or more circles touches the boundary of J^2 . A new overflow then occurs, changing s . Thus, any state within the set of m maximum-size circles is associated with the same s .

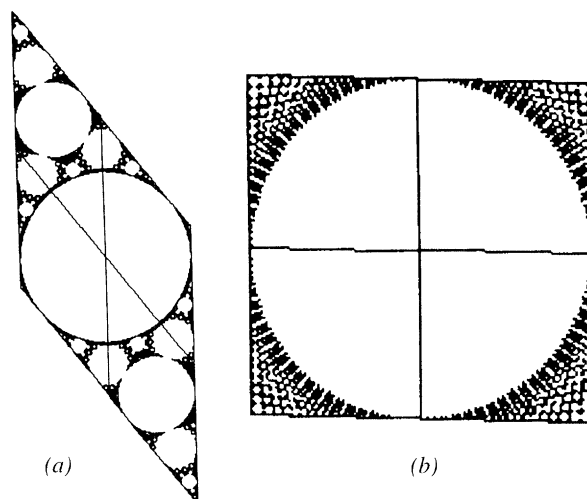


Figure 6. Complex oscillation: (a) $r = 1$, $\theta = 37.86^\circ$, $x_0 = [0.39, -0.39]^T$; (b) $r = 1$, $\theta = 88^\circ$, $x_0 = [0.84, -0.84]^T$.

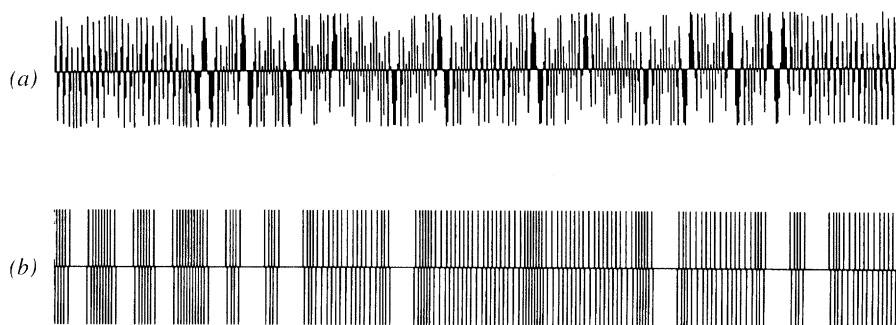


Figure 7. (a) Discrete-time waveform corresponding to figure 6a. (b) Ternary overflow sequence, s , corresponding to figure 6a.

(b) Complex and fractal overflow oscillations

Figure 6 shows typical complex oscillations. The orbit generated avoids all those regions corresponding to the simpler oscillations and therefore simultaneously reveals (by the white areas) those parts of the state space. Figure 7a shows a small part of the figure 6a oscillation as a discrete-time waveform, and figure 7b shows a small part of the ternary overflow sequence s . Such sequences appear to be non-periodic with chaotic properties. However, the Jacobian of \mathbf{F} is the constant matrix \mathbf{A} , so the Lyapunov exponents are simply the log magnitude of the eigenvalues of \mathbf{A} . For $r = 1$, these exponents are therefore zero, and the trajectories are not strictly chaotic. They are, however, on the boundary of a chaotic regime, since they become positive for $r > 1$ (Kocarev & Chua 1993).

Figure 8 is an expanded plot of the lower part of figure 6a; a self-similarity property is evident, but magnification reveals other intricate features. A small change in θ or w_0 can affect the fine detail. Care is needed to prevent numerical rounding errors influencing the appearance at large magnification. With damping, ($r < 1$),

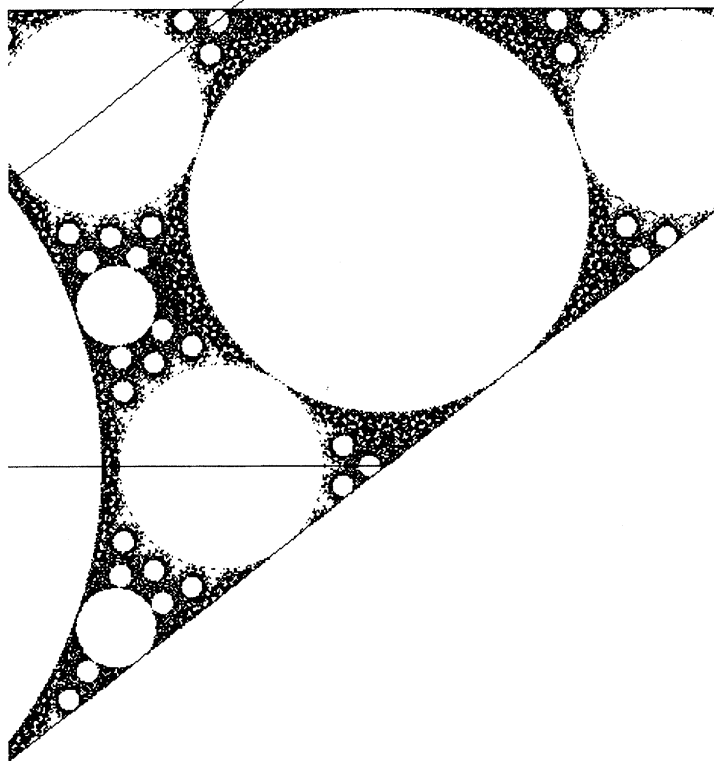


Figure 8. Expansion of part of figure 6a.

discussed further in §7, only periodic limit cycles are observed, although with very small damping, some periods may be very long and their orbit may superficially resemble figure 6a at low resolution.

5. Dynamic structure of the state space

Sufficient conditions for global stability are well known (Ebert *et al.* 1969). Provided that $|a| + |b| < 1$, overflow cannot occur from any state, and so the linear behaviour applies. This defines a square within the stability triangle (figure 1) within which the stable fixed-point $(0,0)$ attracts all trajectories in I^2 and no overflow oscillations can be sustained.

For complex eigenvalues, this is equivalent to the condition,

$$\cos \theta < (1 - r^2)/2r,$$

which defines the shaded area in figure 9. For $r = 1$ and θ/π irrational, overflow oscillations occur for all \mathbf{w}_0 outside the inscribed circle C of the rhombus, while for $r < 1$, they occur only for some \mathbf{w}_0 outside C , if at all.

(a) Periodic sequences

Equations for existence of a period m oscillation are easily derived directly from the state equations, but a solution is practicable only for very short periods (Bose & Chen 1991).

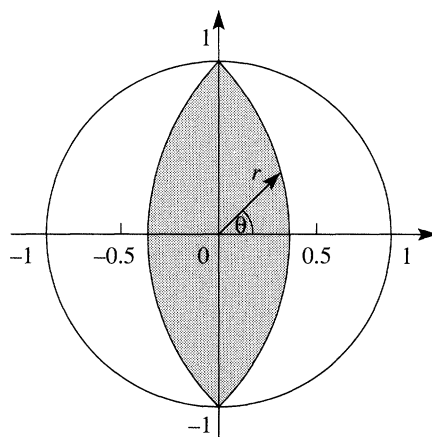


Figure 9. Globally stable region in eigenvalue-plane.

For a ternary sequence $\mathbf{s} = s_0 s_1 s_2 \dots s_{m-1} \dots$ of period m , a corresponding sequence of states $\mathbf{x}_0 \mathbf{x}_1 \mathbf{x}_2 \dots \mathbf{x}_{m-1}$ follows from the state equations by imposing the condition $\mathbf{x}_m = \mathbf{x}_0$:

$$\mathbf{x}_i = [\mathbf{I} - \mathbf{A}^m]^{-1} [\mathbf{A}^{m-1} \mathbf{b} s_i + \mathbf{A}^{m-2} \mathbf{b} s_{i+1} + \dots + \mathbf{A} \mathbf{b} s_{i-2} + \mathbf{b} s_{i-1}]$$

for $i = 0 \dots m - 1$

For $r = 1$, $\det |\mathbf{I} - \mathbf{A}^m| = 2(1 - \cos m\theta) = 4 \sin^2(m\theta/2)$, which is non-zero for irrational θ/π , and the equations have a unique solution. A direct way of testing for the admissibility of a given sequence, \mathbf{s} , is to solve these linear equations and check that all \mathbf{x}_i are in I^2 . If they are, this also proves the existence of the period m oscillation $\mathbf{x}_0 \mathbf{x}_1 \mathbf{x}_2 \dots \mathbf{x}_{m-1}$.

Since there are 3^m sequences of period m (many not admissible) this involves extensive computation even for small m . For $r = 1$, much simpler necessary and sufficient conditions have been derived (Chua & Lin 1990a, b; Galias & Ogorzałek 1992) and if in addition, $\cos \theta$ is rational (so that \mathbf{A} is a rational matrix), Wu & Chua (1993) have shown how the testing may be done using integer arithmetic only, so eliminating rounding errors. For this condition 2^m is an upper bound for the number of period m sequences. Many properties of admissible sequences have been found, though most are for specific values of θ only. For $\theta < \pi/2$, Wu & Chua (1993) have shown that only the period-2 sequence $(+, -, +, -, \dots)$ is without zeros, and that no sequence can have two adjacent overflows in the same direction (e.g. subsequences containing $+, +$ or $-, -$ are inadmissible in this range of θ).

Although these approaches enable non-admissible and admissible sequences to be catalogued for small m and specific θ values, they do not offer a general solution or means of investigating long period and complex oscillations.

(b) Consequences of the uniqueness of predecessors

For $r \leq 1$, no \mathbf{w} within C can be on a trajectory leading out of C , and so cannot be on an overflow oscillation. For $r < 1$, all \mathbf{w} within C , and some outside, lead to the stable fixed-point at the origin.

Since no state can be simultaneously on more than one oscillation, the state space is partitioned into distinct regions, each one associated with a particular overflow sequence.

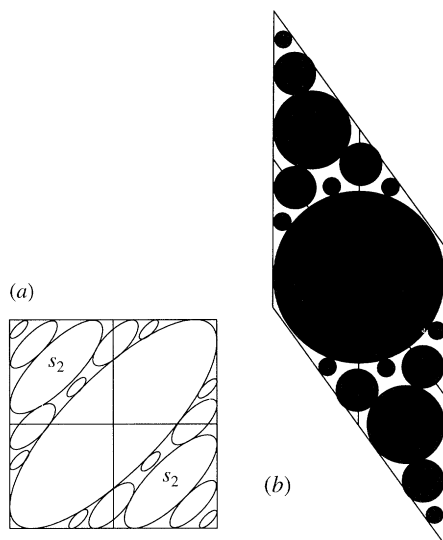


Figure 10. Area occupied by simple oscillations for $\theta = 37.86^\circ$ in x and w -planes.

Because of the uniqueness of state predecessors, for $r = 1$ no w outside C can be on a trajectory which leads into C because each w in C has its immediate predecessor within C . The interior of C consists of just those w where the behaviour is linear with no overflows. For $r = 1$ any w outside C must therefore be on some overflow oscillation which forms a closed loop of states (maybe infinite in number), remaining permanently outside C .

6. Analysis of the lossless case

In the lossless case with $\theta < \pi/2$, Davies (1992) showed that a class of simple oscillations with exactly one + and - element in adjacent positions in each period of s exists if and only if the period, m , is in the range $2 \leq m < \text{Int}(\pi/\theta)$. These oscillations form a simple pattern of $m - 1$ ellipses on one side of the origin and one on the opposite side. In J^2 the ellipses become circles, and the centres and maximum radii of the circles can be derived analytically. Figure 4a is such an oscillation.

For example, if $36^\circ < \theta < 45^\circ$ the overflow-sequences in this class are:

$$\begin{aligned}
 s2 & : \quad +, -, +, -, +, -, +, -, \dots && (\text{period } 2), \\
 s3A & : \quad +, -, 0, +, -, 0, +, -, 0, \dots && (\text{period } 3), \\
 s3B & : \quad -, +, 0, -, +, 0, -, +, 0, \dots && (\text{period } 3), \\
 s4A & : \quad +, -, 0, 0, +, -, 0, 0, +, -, 0, 0, \dots && (\text{period } 4), \\
 s4B & : \quad -, +, 0, 0, -, +, 0, 0, -, +, 0, 0, \dots && (\text{period } 4).
 \end{aligned}$$

Figure 10 shows the maximum-size circles of all these oscillations and the overflow-free area for $\theta = 36.87^\circ$. In J^2 , there is always one circle on the long diagonal of the rhombus, with centre at the point (w_1, w_2) given by

$$w_1 = 1 - \cot \frac{1}{2}m\theta \tan \frac{1}{2}\theta; \quad w_2 = -\sin \frac{1}{2}(m-1)\theta / \sin \frac{1}{2}\theta \sin \frac{1}{2}m\theta.$$

The maximum radius, r_m , of this circle is $1 - w_1$, and since there are m circles for

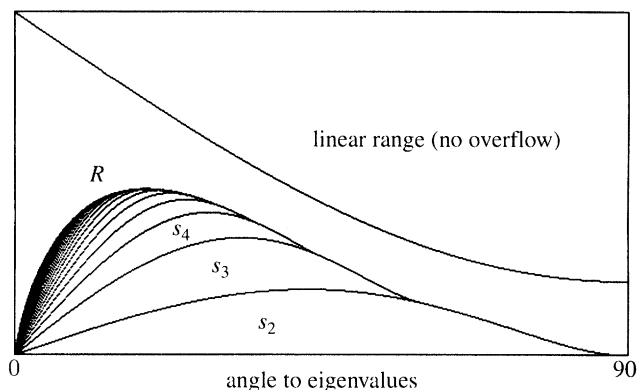


Figure 11. Variation in area occupied by each of the simple oscillations.

period m , they occupy a total area of $m\pi r_m^2$. The variation of area with θ follows a similar pattern in each case. As θ is increased from 0, the area grows, reaches a maximum, and then reduces to zero when $m = \text{Int}(\pi/\theta)$. The I^2 coordinates (x_1, x_2) are $(w_1, -w_1)$.

The area taken up by all oscillations is the rhombus area minus the area of C . The residue, R , left after removing all circles of this class of simple oscillations is given by

$$R = \frac{4}{\sin \theta} - \pi - 2\pi r_2^2 - 2 \sum_{m=3}^{\text{Int}(\pi/\theta)} m\pi r_m^2.$$

Figure 11 shows how the number of different periods changes with θ . As θ is reduced from $\pi/2$, the two circles corresponding to s_2 increase in size to a maximum then decrease. The six circles corresponding to s_3A and s_3B are created when $\pi/3$ is reached then grow and shrink again. Similarly the eight circles of s_4A and s_4B are created at $\pi/4$, and so on. R is the area available for other oscillations, including short-period ones such as a period-3 sequence $\dots 00+\dots$ admissible for $\pi/3 < \theta < \pi/2$ and the period-17 sequence shown in figure 4*b* as well as all the complex ones with fractal appearance.

These results reveal a part of the structure of the state space: by removing the space occupied by simple oscillations (the black part of figure 10) the residue becomes increasingly fragmented. Any oscillation with a long-period s which remains in this residue must inevitably have a complex structure, in order to avoid parts already accounted for. For $\theta > \pi/2$, the character of the admissible sequences is generally quite different, and has not been investigated so thoroughly.

An oscillation comprising a finite number of ellipses corresponds to a periodic admissible sequence with period equal to the number of ellipses so I^2 may be partitioned according to the character of the oscillations in each region. Three sets of ternary sequences $\Sigma_\alpha, \Sigma_\beta, \Sigma_\gamma$, may be defined as follows:

- Σ_α : s has finite period,
- Σ_β : s has finite period following an initial transient,
- Σ_γ : s is not periodic.

Then $I_\alpha = S^{-1}(\Sigma_\alpha \cap \Sigma_F)$ is the subset of I^2 which contains the states on oscillations

comprising a finite number of ellipses. Chua & Lin (1988) show that $I_\beta = S^{-1}(\Sigma_\beta \cap \Sigma_F)$ corresponds to oscillations which must start on the boundary $x_1 = 1$ or $x_2 = 1$ and continue on the boundaries of a set of ellipses whose interior is in I_α .

The topology of the remaining area $I_\gamma = S^{-1}(\Sigma_\gamma \cap \Sigma_F) = I^2 - (I_\alpha \cup I_\beta)$ has been investigated by Wu & Chua (1993) with conclusions that points in I_γ comprise line segments and that if there is a finite number of admissible sequences in $\Sigma_\alpha \cup \Sigma_\beta$ then there is an uncountable number in Σ_γ .

Since a real digital filter cannot have states with $x_1 = 1$ or $x_2 = 1$, it therefore has no oscillations in I_β . In a simulation or practical realization of a digital filter, those oscillations with states in I_α and which consist of many small ellipses are indistinguishable from oscillations in I_γ .

7. The behaviour with damping

At each transition, the distance of the state from the origin in J^2 shrinks by r , unless accompanied by an overflow. Overflow oscillations which, for $r = 1$, would form two or more circles in J^2 , converge towards limit cycles, which for small damping, are a sequence of states close to the centres of the circles, with the same period as the ternary overflow sequence \mathbf{s} . Thus J^2 comprises these periodic attractors surrounded by basins of attraction which, for very small damping, include regions similar to the maximum-diameter circles of the lossless case. As r is reduced, the states of each limit cycle move away from the centres of the $r = 1$ circles, and their basins of attraction acquire a more irregular shape with other parts of J^2 added. Longer-period cycles cease to be sustainable. Eventually, the whole of J^2 is the basins of attraction of the fixed point at the origin and the period-2 limit cycle associated with $\mathbf{s} = \{+, -\}$. Finally, the filter becomes globally stable with a single attractor.

Thus as r is decreased from unity, there is a progressive disappearance of long-period oscillations, the ones that remain being those associated with ternary overflow sequences which can produce large circles in the lossless case. The larger the circles associated with an $r = 1$ oscillation the more robust these oscillations are against reduction in r or changes in θ . This provides a qualitative outline of the behaviour.

For negative damping (e.g. $r > 1$), the structure is linearly unstable, and all states in C are on outward-moving trajectories, eventually leading to overflow.

Such oscillations show promise as pseudo-random signal sources, with scope for controlling the statistical properties by changing the filter-coefficients (Kutzer & Schwarz 1994; Kutzer *et al.* 1994). By contrast with $r \leq 1$, the behaviour for $r > 1$ is not critically dependent upon the initial state, which is advantageous for a practically useful signal source. Particular cases of linearly unstable structures with integer coefficients are equivalent to a sawtooth map, for which several kinds of well-documented chaotic behaviour can occur (Kocarev *et al.* 1994b).

8. Finite wordlength of signals

Because signals in a real digital filter are quantised, there is a finite number of states (e.g. for a second-order filter with 16-bit signal wordlength, there are 2^{32} states). The zero-input response of any finite-state machine is periodic, so all overflow oscillations are periodic. The complex oscillations can thus never be more than

pseudo-chaotic in practice although the period may be long enough for them to be useful pseudo-random signals.

For $r = 1$, the complex sequences occur only in R (figure 10), which has to support many different sequences. The maximum period is therefore much less than the total number of states. Lin & Chua (1993) found that when $b = -1$ and a is a power of two, no period exceeded 2,495 for 8-bit quantization, and none exceeded 815 747 for 15-bit quantization (compared with total states of 65 536 and 2^{30} respectively).

9. Higher order digital filters

Some investigations of third-order filters have been reported (Chua & Lin 1990*a*; Kutzer 1994). The state space is the cube $I^3 : -1 \leq x_1, x_2, x_3 < +1$ and the behaviour correspondingly more complicated. Third-order digital filters provide more choice of coefficient values and as a source of pseudo-random signals promise a greater variety of statistical properties than is available from second-order filters (Kutzer & Schwarz 1994). For example, coefficients can be chosen to provide a signal with a uniform probability density function and a flat frequency spectrum. An eigenvalue analysis of the nonlinear dynamics of the n th-order direct-form filter has been given by Kocarev *et al.* (1994).

10. Other overflow nonlinearities

The two's complement nonlinearity is in practice normally replaced by a saturation nonlinearity (an overflowed state variable is set to the maximum value), for which no oscillation can occur with a linearly stable second-order filter, or occasionally by a zeroing nonlinearity (an overflowed state variable is set to zero). In the former case complex and chaotic behaviour can occur for a linearly unstable filter (Kocarev *et al.* 1994*b*). Rakhmanova *et al.* (1994) have investigated the latter case and derived existence conditions for oscillations.

11. Conclusions

The mechanism which causes overflow oscillations in digital filters and approaches to its mathematical analysis have been described. The variation in behaviour with location r, θ of the complex eigenvalues has been emphasized. The transformed state space J^2 is convenient for investigating the behaviour, but unsolved problems remain such as admissibility of overflow sequences, the detailed structure of the complex fractal-like oscillations from lossless resonators, the shapes of the basins of attraction with damping, and the periodic lengths achievable for finite-wordlength signals. Possible applications have only recently begun to be investigated.

Georgi Petkov is thanked for assistance with the preparation of this paper and the UK Engineering and Physical Sciences Research Council (Grant GR/J 16459) and the British-German ARC programme (Project 393) are thanked for financial support.

Appendix A. The uniqueness of state predecessors for $r \leq 1$

Consider two states \mathbf{x}'_k and \mathbf{x}''_k , followed by overflow s'_k, s''_k respectively, and suppose that they have the same successor \mathbf{x}_{k+1} .

$$\begin{aligned}x_{1(k+1)} &= x'_{2(k)} = x''_{2(k)}, \\x_{2(k+1)} &= -r^2 x'_{1(k)} + 2r \cos \theta x'_{2(k)} + 2s'_k \\ &= -r^2 x''_{1(k)} + 2r \cos \theta x''_{2(k)} + 2s''_k.\end{aligned}$$

Therefore $x'_{1(k)} - x''_{1(k)} = 2/[r^2(s'_k - s''_k)]$, so

$$x'_{1(k)} - x''_{1(k)} \in \{0, \pm 2/r^2, \pm 4/r^2\}.$$

Since $-1 \leq x_k < 1$, $|x'_{1(k)} - x''_{1(k)}| < 1$ and so $x'_{1(k)} = x''_{1(k)}$ if $r \leq 1$.

Consequently, no state can have more than one predecessor for $r \leq 1$. There are pathological cases where a state has no predecessor: for example, if $r = 0$, \mathbf{A} is singular, and a state with non-zero x_2 cannot follow any other state. Otherwise each state has one predecessor.

References

- Barnes, C. W. & Fam, A. T. 1977 Minimum-norm recursive digital filters that are free of overflow limit cycles. *IEEE Trans. Circuits Syst.* **CAS-24**, 569–574.
- Bose, T. & Chen, M.-Q. 1991 Overflow oscillations in state space digital filters. *IEEE Trans. Circuits Syst.* **CAS-38**, 807–810.
- Butterweck, H.-J., Ritzerfeld, J & Werter, M. 1989 Finite wordlength effects in digital filters. *IEEE Trans. Circuits Syst.* **CAS-24**, 76–89.
- Chua, L. O. & Lin, T. 1988 Chaos in digital filters. *IEEE Trans. Circuits Syst.* **CAS-35**, 648–658.
- Chua, L. O. & Lin, T. 1990a Chaos and fractals from 3rd order filters. *Int. J. Circuit Theory Applic.* **18**, 241–255.
- Chua, L. O. & Lin, T. 1990b Fractal pattern of second order nonlinear digital filters. *Int. J. Circuit Theory Applic.* **18**, 541–550.
- Chua, L. O. & Lin, T. 1991 On chaos of digital filters in the real world. *IEEE Trans. Circuits Syst.* **38**, 557–558.
- Davies, A. C. 1992 Geometrical analysis of digital-filter overflow oscillations. *Proc. IEEE Symp. Circuits and Systems, San Diego*, pp. 256–259.
- Davies, A. C. 1994 Digital filter overflow – explaining the fractal. *Proc. Int. Workshop on Nonlinear Dynamics of Electronic Systems, Kraków, Poland*, pp. 73–78.
- Davies, A. C. & Sriranjjan, R. 1989 Chaotic signals generated by overflow nonlinearities in digital filters. *IEE Saraga Colloquium Digest, London*, 8/1–8/6.
- Ebert, P. M., Mazo, J. E. & Taylor, M. G. 1969 Overflow oscillations in digital filters. *Bell Syst. Tech. J.* **48**, 2999–3020.
- Galias, Z. & Ogorzałek, M. J. 1992 On symbolic dynamics of a chaotic second-order digital filter. *Int. J. Circuit Theory Applic.* **20**, 401–409.
- Kocarev, L. & Chua, L. O. 1993 On chaos in digital filters: case $b = -1$. *IEEE Trans. Circuits Syst. II. Analog Digital Signal Processing* **40**, 404–407.
- Kocarev, L., Ogorzałek, M. J. & Ribarov, K. 1994 Chaotic behaviour in n th order digital filters. In *Proc. Int. Workshop in Nonlinear Dynamics of Electronic Systems, Kraków, Poland*, pp. 203–208.

- Kocarev, L., Wu, C. W., Chua, L. O., Galias, Z. & Orgozalek, M. 1994 Chaos in digital filters: a global picture. In *Systems and networks: mathematical theory and applications* (ed. U. Helmke *et al.*), pp. 299–307. Berlin: Akademie.
- Kutzer, K. 1994 Geometrical analysis of the behaviour of third-order digital filters. In *Nonlinear dynamics of electronic systems* (ed. A. C. Davies *et al.*), pp. 155–162. Singapore: World Scientific.
- Kutzer, K. & Schwarz, W. 1994 Noise generator design based on digital filters. In *Proc. Int. Workshop in Nonlinear Dynamics of Electronic Systems, Kraków, Poland*, pp. 209–214.
- Kutzer, K., Schwarz, W. & Davies, A. C. 1994 Chaotic signals generated by digital filter overflow. *Proc. IEEE Symp. Circuits and Systems, London*, 6/17–6/20.
- Laakso, T. I. 1993 Elimination of limit cycles in direct form digital filters using error feedback. *Int. J. Circuit Theory Applic.* **21**, 141–163.
- Lin, T. & Chua, L. O. 1993 A new class of pseudo-random number generator based on chaos in digital filters. *Int. J. Circuit Theory Applic.* **21**, 473–480.
- Ogorzałek, M. J. 1992 Complex behaviour in digital filters. *Int. J. Bifurc. Chaos* **2**, 11–29.
- Ogorzałek, M. J., Hasler, M. & Boite, R. 1992 Chaos in recursive digital filters. *Signal Processing VI*, pp. 191–194. Elsevier.
- Rakhmanova, N. K., Rakhmanov, A. I., Fedorenko, V. V. & Sharkovskii, A. N. 1994 Dynamics of digital filter with zeroing type piece wise linear characteristic. In *Proc. Int. Workshop in Nonlinear Dynamics of Electronic Systems, Kraków, Poland*, pp. 67–71.
- Roberts, R. A. & Mullis, C. T. 1987 *Digital signal processing*, §9.3. Reading, MA: Addison Wesley.
- Wu, C. W. & Chua, L. O. 1993 Properties of admissible symbol sequences in a second-order digital filter with overflow nonlinearity. *Int. J. Circuit Theory Applic.* **21**, 299–307.